Review

Author for correspondence:
Anowar J. Shajib
e-mail: ajshajib@uchicago.edu

†NHFP Einstein Fellow.

THE ROYAL SOCIETY
PUBLISHING

Strong gravitational lenses from the Vera C. Rubin Observatory

Anowar J. Shajib[1,2,3,†], Graham P. Smith[4], Simon Birrer[5], Aprajita Verma[6], Nikki Arendse[7], Thomas Collett[8], Tansu Daylan[9], Stephen Serjeant[10], LSST Strong Lensing Science Collaboration

[1]Department of Astronomy and Astrophysics, [2]Kavli Institute for Cosmological Physics, University of Chicago, Chicago, IL, USA
[3]Center for Astronomy, Space Science and Astrophysics, Independent University, Bangladesh, Dhaka 1229, Bangladesh
[4]School of Physics and Astronomy, University of Birmingham, Birmingham B152TT, UK
[5]Department of Physics and Astronomy, Stony Brook University, Stony Brook, NY 11794, USA
[6]Sub-department of Astrophysics, University of Oxford, Oxford OX13RH, UK
[7]Department of Physics, The Oskar Klein Centre, Stockholms Universitet, Stockholm, Sweden
[8]Institute of Cosmology and Gravitation, University of Portsmouth, Portsmouth, Hampshire PO13FX, UK
[9]Department of Physics, McDonnell Center for the Space Sciences, Washington University in St Louis, St Louis, MO 63130, USA
[10]School of Physical Sciences, The Open University, Milton Keynes MK76AA, UK

AJS, 0000-0002-5558-888X; GS, 0000-0003-4494-8277; SB, 0000-0003-3195-5507; TD, 0000-0002-6939-9211

Like many areas of astrophysics and cosmology, the Vera C. Rubin Observatory will be transformational for almost all the applications of strong lensing, thanks to the dramatic increase in the number of known strong lenses by two orders of magnitude or more and the readily available time-domain data for the lenses with transient sources. In this article, we provide an overview of the forecasted number of discovered lenses of different types and describe the primary science cases these large lens samples will enable. We provide an updated forecast on the joint constraint for the dark energy equation-of-state parameters, w_0 and w_a, from combining all strong-lensing probes of dark energy. We update the previous forecast

from the Rubin Observatory Dark Energy Science Collaboration's Science Review Document by adding two new crucial strong-lensing samples: lensed type Ia supernovae and single-deflector lenses with measured stellar kinematics. Finally, we describe the current and near-future activities and collaborative efforts within the strong-lensing community in preparation for the arrival of the first real dataset from Rubin in 2026.

This article is part of the Theo Murphy meeting issue 'Multi-messenger gravitational lensing (Part 2)'.

1. Introduction

The Vera C. Rubin Observatory's Legacy Survey of Space and Time (LSST) is a ground-based, time-domain, imaging survey in the optical, which will cover 18 000 square degrees and will operate for 10 years [1]. This survey will deliver unprecedented data and impact for many areas in astrophysics and cosmology [2]. The field of strong lensing is also set to experience a revolutionary advancement given the increase of known strong lenses to increase by two orders of magnitude or more, thanks to the Rubin LSST and other concurrent large-area sky surveys such as *Euclid* and the *Roman* Space Telescope [3–5]. Furthermore, the lenses with time-variable sources will have readily available light curves from the LSST to enable several strong-lensing science applications without requiring follow-up monitoring. Strong-lensing systems have many applications in astrophysics and cosmology, each of which will benefit from such a dramatic increase in known systems.

This article overviews some of the main strong-lensing science cases to be achieved with the Rubin data. It is intended to summarize the science cases rather than provide a detailed review of the methodologies used to accomplish each science goal from the data. However, we refer the readers to comprehensive review articles for the science cases described, with the references provided within relevant sections.

This article is organized as follows. In §2, we provide a brief review of the estimates for discoveries of different types of lens systems, e.g. lensed quasars, lensed supernovae (SNe), galaxy–galaxy lenses. Then, in §3, we describe the main science goals in the field of strong lensing to be accomplished with the Rubin samples. We then describe the current and near-future efforts within the strong-lensing community in preparation for the real Rubin dataset (Data Preview 2) to arrive in 2026 in §4.

2. Forecasts for lens discoveries

The Rubin Observatory LSST will catalogue 20 billion galaxies after its 10-year survey.[1] After only 1 year of the survey, the total size of the catalogue will surpass that of all previous surveys combined. Such a drastic increase in the number of objects will also be reflected in the size of known strong-lensing systems. Indeed, Collett [4] predicts 1 20 000 galaxy-scale lenses to be discovered from the LSST 10-year survey with optimal image stacking, providing two orders of magnitude increase in the number of known galaxy–galaxy lenses (figure 1). For the conservative case of lens finding that requires blue-red difference imaging, this number comes down to 62 000 galaxy-scale lenses, still a field-changing number. However, as the LSST will be seeing-limited, the expected strong lens sample will have an Einstein radius distribution that peaks around 1″, missing very small-separation lenses. While it will be a huge challenge to identify $\mathcal{O}(10^5)$ lenses among $\mathcal{O}(10^{10})$ Rubin galaxies, machine-learning-based search algorithms [6–8] and citizen science [9] combined with ensemble classifiers [10] may be up to the challenge.
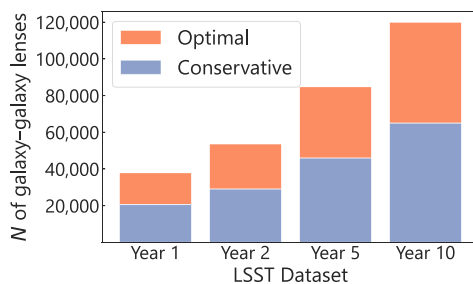
---

[1]https://rubinobservatory.org/explore/numbers

Figure 1. Forecasted number of galaxy–galaxy lenses to be discovered by the Rubin LSST [4]. The numbers for the Year-10 dataset are the directly forecasted ones, and those for the intermediate years are scaled with the imaging signal-to-noise ratio, simply assuming a uniform coverage and cadence, given that the number of discovered lenses linearly scales with the imaging signal-to-noise ratio [4]. The heights of the orange bars show the forecasted numbers for the scenario with optimal image stacking ([4], for definition). The heights of the blue bars represent the 'conservative' case where lens finding requires blue-red difference imaging. Year 1−2 datasets will already provide a large fraction (30−45%) of the total discoverable lenses with the full 10-year dataset.

Lensed SNe with galaxy-scale deflectors can be an alternative avenue to detect small-separation lenses if discovered through magnification selection. For example, the only two galaxy-scale lensed SNe, iPTF16geu and SN Zwicky, are both small-separation lenses ($\theta_E \sim 0.17'' - 0.3''$) [11,12]. From its 10-year survey, LSST is expected to discover approximately 380 such unresolved lensed SNe [13], approximately 180 of which would be type Ia [14]. In a separate forecast, Wojtak *et al.* [15] consider discovery methods for both resolved and unresolved lensed SNe and predict 3400 lensed SNe, a much higher number, to be discovered by the LSST. Arendse *et al.* [16] have performed a detailed study on the effect of different cadence strategies (e.g. rolling[2] versus non-rolling) on the number of discovered lensed SNIa to find that this number, 44 per year, is largely unaffected by this choice.

For lensed quasars at the galaxy scale, the mock catalogue of [3] forecasts 3132 systems[3] to be discovered after 10 years, with a quad fraction of 15%. From this sample, Taak & Treu [17] forecast that approximately 1000 lensed quasars will have variability above the LSST photometric uncertainty, making the time delay measurable for use in time-delay cosmography from the LSST light curves alone. They [17] additionally demonstrate that a smaller sample of approximately 250 lenses will have much larger variability for the time delays to be measurable with higher cadence monitoring with smaller 2−4 m class telescopes. Yue *et al.* [18] provide a new mock catalogue of lensed quasars using recently obtained empirical quasar luminosity functions and the CosmoDC2 mock catalogue for the deflector population, forecasting 2377 lensed quasars with 193 quads among them. If this mock catalogue of [18] is used instead of the one from [3], the forecasted numbers of systems with measurable time delays from [17] could be lower by a factor of approximately 5.

The above forecasts were carried out mostly for galaxy-scale lenses, given their relatively simpler population statistics than group- and cluster-scale deflectors. However, qualitatively, the Rubin LSST can be expected to deliver a similar increase by one order of magnitude or more in the number of known group- and cluster-scale lenses [19].

3. Strong-lensing science cases with Rubin

In this section, we summarize some of the main science goals for strong lensing with the Rubin data or Rubin-discovered lens samples: (i) measuring cosmological parameters; (ii) studying

---

[2]For a description, see https://pstn-055.lsst.io/
[3]All the forecasted numbers in this paragraph correspond to a 20,000 square degree LSST coverage as assumed by [17] and [18].

dark matter microphysics; (iii) studying galaxy evolution at both intermediate ($z \lesssim 1$) and high redshifts ($z \gtrsim 2$); and (iv) studying the structure and physics of transient events. However, this is not a comprehensive list of all the science questions that strong lensing can help answer. The unprecedented increase in the number of known strong lenses delivered by the Rubin LSST will undoubtedly help all the strong-lensing science applications.

(a) Measuring cosmological parameters

Strong lenses can act as a cosmological probe in several ways. First, the time delay between the multiple lensed images carries cosmological information [20]. This probe is primarily sensitive to the Hubble constant but also weakly depends on other cosmological parameters that govern late-time expansion history ([21,22], for some recent reviews). The time delay can be measured when the background source is either variable or transient. So far, this technique has been applied on eight lensed quasars at the galaxy scale by the Time-Delay COSMOgraphy (TDCOSMO) collaboration [23,24] and on three lensed quasars (with time delays measured for six image pairs) on the galaxy-cluster scale [25]. Strongly lensed SNe are much rarer than lensed quasars, with the first such system only being discovered in the 2010s [11,26,27]. Only two lensed SNe have been used for cosmographic measurements, both at the cluster scale [28,29]. Although the JWST has been impactful in discovering a handful of lensed SNe in recent years [30], they are serendipitous, and this rate of discovery is not guaranteed to continue in the future. The LSST provides a stable channel for discovering lenses SNe at all deflector scales and will provide a more easily characterizable selection function. We note that to fully harness the cosmological information of the time-delay lenses from the Rubin LSST, follow-up data with other facilities, such as high-cadence monitoring for more precise time delays, high-resolution imaging and spatially resolved stellar kinematics, will be necessary [31–34].

Second, double-source-plane lenses provide a way to constrain a ratio β of angular diameter distances (D) given by

$$\beta \equiv \frac{D_{ds1} D_{s2}}{D_{s1} D_{ds2}}, \tag{3.1}$$

where d, s1 and s2 in the subscripts of D denote the deflector, source 1 and source 2, respectively [35]. Although this ratio is insensitive to the Hubble constant, it is sensitive to the density parameters and the dark energy equation-of-state parameters [36–38]. While many cluster-scale lenses have been discovered with ≥ 2 source planes ([39], for a review), only a handful of double-source-plane galaxy-scale lenses are known so far [40–42]. However, Rubin LSST is expected to deliver a sample of $\mathcal{O}(10^2)$ double-source-plane galaxy-scale lenses [43]. The advantage of galaxy-scale lenses is that their mass distributions are more straightforward to model than group-scale or cluster-scale lenses.

Third, all galaxy-scale lenses, including single-plane ones, with measured kinematics constrain the distance ratio D_s/D_{ds}, where D_s is the angular diameter distance to the source and D_{ds} is the angular diameter distance between the deflector and the source. Thus, constraining this ratio also allows for measuring the density parameters and the dark energy equation-of-state parameters. Li *et al.* [44] have forecasted competitive precisions on the cosmological parameters from a sample of 10 000 galaxy-scale lenses (hereafter, single-plane lenses) to be discovered by future surveys such as the LSST, for which single-aperture stellar kinematics would be measured with the 4MOST Strong Lensing Spectroscopic Legacy Survey [45].

In this article, we forecast the joint constraint from the above dark energy probes on the equation-of-state parameters, w_0 and w_a, to be delivered by Rubin LSST samples and follow-up data collected with other facilities. In this forecast, we make a few updates on the previous forecast provided by [43]. First, we include time-delay cosmography with lensed SNIa, for which the mass-sheet degeneracy can be broken with measured magnifications [46]. Second, we include the sample of single-plane lenses with kinematics from [44]. Third, we adopt the number
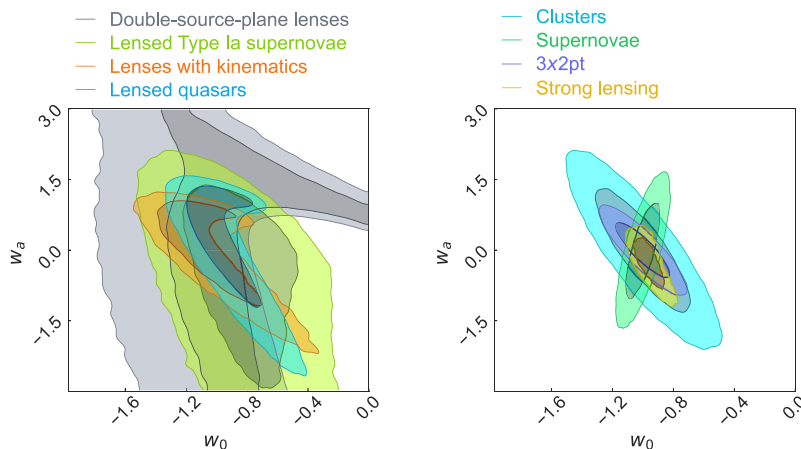
Figure 2. The forecasted constraints on the w_0–w_a plane from LSST 10-year dataset. Left-hand panel: Individual constraints from the four strong-lensing probes. The particular shape of degeneracy for a given strong-lensing probe originates from using the particular ratio(s) of angular diameter distances to constrain the cosmological parameters. Right-hand panel: Forecasted joint constraints from combining the four strong-lensing probes (yellow), in comparison with three other cosmological probes of Rubin: clusters (cyan), supernovae (green), and 3×2 pt correlations (blue). The figures of merit [49] for these probes are 11, 32 and 48, respectively. The figure of merit for the combined strong-lensing probes is 69, making it the most constraining probe of the dark energy from the Rubin LSST.

of lensed quasar systems with measured time delays to 236 based on [17] and assume 40 of these systems will have spatially resolved kinematics measured with the *JWST* integral field spectroscopy [47]. We allow the mass-sheet degeneracy to be broken with the kinematic data for the galaxy–quasar lenses, with full covariance accounted for within the time-delay cosmography sample consisting of lensed quasars and SNIae. We use the same sample of 87 lenses from the mock sample of double-source planes from [43,48]. We provide additional specifications and settings of the forecast in appendix A. We show the forecast for individual probes and compare the joint-strong-lensing forecast with other cosmological probes of the LSST in figure 2. The combined strong-lensing probe will provide the strongest constraint on the dark energy parameters among the Rubin LSST probes, including 3×2 point correlations, SNe and clusters, based on their current forecasts [43]. Combining strong-lensing constraints with those from the other independent probes will constrain the dark energy parameters even tighter due to the orthogonality of the contours.

A caveat of this forecast is that it does not account for correlated systematics between the time-delay cosmography sample and the single-plane lenses. Although accounting for correlated modelling systematics can potentially increase the forecasted uncertainty, the large sample of single-plane lenses with measured kinematics, in turn, can effectively constrain the mass-sheet degeneracy more tightly [24]. This degeneracy can be broken even more effectively if stacked galaxy–galaxy weak lensing measurements for this large sample of single-plane lenses are also used [50]. Thus, this sample of single-plane lenses may either increase the constraining power of the time-delay cosmography sample or alleviate the need for relatively expensive spatially resolved stellar kinematics measurement. A detailed exploration of the trade-off between these two counteracting effects is left for a future study.

(b) Dark matter microphysics

Strong lensing can be used to explore how dark matter is structured at small scales, which yields a strong probe of the particle nature of dark matter. The abundance, spatial distribution and *N*-point correlation of dark matter substructure in the halo of lensing galaxies differ for different

theories of dark matter, such as cold and warm dark matter ([51], for a review). These substructures can be detected by the 'flux-ratio anomaly' in the multiple images [52] or inferring subhalos in the mass model that explains the kinks or perturbations in the lensed arcs or arclets, i.e. the 'gravitational imaging' method [53–56]. Whereas the gravitational imaging technique can lead to degenerate detection between a substructure within the lens's halo and a line-of-sight halo [57], the line-of-sight halos can increase the sensitivity of probing the subhalo mass function with the flux-ratio anomalies [58]. An alternative method to constrain dark matter microphysics is the power spectrum of dark matter fluctuations [59]. Unlike the millilensing signature accessible to near-diffraction-limited images of the *Hubble* Space Telescope (HST) [60], *Roman* [61] and the JWST [62], the seeing-limited images in LSST will only allow inference of relatively more massive ($M_{\rm sub} \gtrsim 10^{11} M_\odot$) substructure in galaxy clusters. In addition, the statistics of substructures within cluster-scale lenses' halos can also be used to test predictions of the cold dark matter paradigm ([63], for a review). The current limitation of these methods is the number of confirmed strong lenses with high signal-to-noise ratios amenable to detailed characterization that can reveal population-level properties across cosmic time while controlling for system-to-system variance. The Rubin LSST is expected to increase the sample size by an order of magnitude.

Another path to explore the microphysics of dark matter is through the shape of dark matter halos [64,65]. The 'core-cusp' problem still poses a challenge for the cold dark matter paradigm [66,67], for which galaxy-scale strong lenses can provide key insights, especially for the massive elliptical deflector galaxies that will be detected in abundance by the LSST. In addition, Rubin LSST is expected to discover lenses with dwarf galaxy deflectors, which can be used to probe their halo shape [68], providing valuable constraints in a relatively understudied mass regime. Additionally, microlensing can be used to constrain the dark matter fraction made of compact objects, such as primordial black holes [69,70].

(c) Galaxy evolution

Strong-lensing systems allow studying galaxy evolution in two avenues. First, strong lensing is one of only a handful of probes of the mass distribution in (deflector) galaxies. Thus, we can study the structural evolution of the deflectors shaped by baryonic feedback processes and mergers ([71], for a review). Additionally, comparing the stellar mass measured with lensing-dynamics analysis to that obtained using stellar population synthesis also allows the stellar initial mass function and its evolution to be constrained. Whereas some results from this method in the literature have conflicted [71], the unprecedentedly large lens sample from the LSST holds promise to resolve the conflicts if they originated from a small sample size, unaccounted for or non-uniform selection function, or not accounting for correlation with other galaxy properties due to a combination of both of the former reasons.

Second, strong lensing acts as a 'natural telescope' magnifying distant background galaxies ([63], for a review at the cluster scale). Thus, the structure and spatial properties of these galaxies can be studied at higher spatial resolution compared to unlensed galaxies at the same redshift. Current 10m-class and future extremely large telescopes will play a critical role in such studies. These magnified high-redshift galaxies can, therefore, be used not only for uncovering the impact of baryon cycling in their evolution but also to provide an important avenue to answer key questions about cosmic reionization at the highest redshifts [72]. The large samples of lenses discovered by the Rubin LSST will constrain galaxy properties and their evolution to high precision, both for the deflector and source populations.

(d) Structure and physics of transients

The structure and physics of lensed transient sources can be studied through microlensing, i.e. additional magnification or demagnification of a lensed image due to lensing by stars in the foreground lensing galaxy. Microlensing-induced signatures, in the form of 'anomalous' flux ratios

between multiple images relative to that expected in the absence of microlensing, long-term variability of the flux ratio, or departure from well-modelled SNe light curve shapes, can be identified in the light curves of the images. These signatures allow the structure of the transient source to be probed, for example, the quasar accretion disk or SN photosphere ([73,74], for reviews). In addition, the statistics of microlensing events probe the stellar IMF in the lensing galaxies [75]. Thanks to its time-domain nature, Rubin LSST will readily provide light curves of these lensed transients, enabling the long-term variability induced by microlensing to be constrained. These light curves will also contain ~300 per year high-magnification events with much stronger constraining power [76]. Additionally, these light curves can help identify the onset of high-magnification events for higher-cadence monitoring with independent follow-up facilities, with such closely monitored events having been only a handful so far [73].

In addition to the transients mentioned above, strongly lensed gamma-ray bursts, fast radio bursts, kilonovae and gravitational wave events would be immensely helpful in uncovering the underlying astrophysical mechanisms in these transient events [77]. For detecting and confirming the lensing nature of these transients, cross-referencing with a catalogue of known lensing objects is a highly promising avenue [78,79]. The Rubin LSST will effectively provide the largest such catalogue of lensing systems for this purpose.

4. Ongoing and near-future community efforts

The strong-lensing community activities are carried out unitedly by two collaborations: the Strong Lensing Science Collaboration[4] (SLSC) and the Dark Energy Science Collaboration[5] (DESC) through its Strong Lensing Topical Team (SLTT).[6] The coordination and exchange of expertise and resources are mutually agreed upon through an official memorandum of understanding.

In preparation for the first light and soon-to-be-delivered first dataset (Data Preview 2 in 2026) from the Rubin LSST, SLSC and DESC-SLTT are jointly contributing to commissioning Rubin's active optics sub-system and alert production pipeline[7] [80], and coordinating community efforts in terms of individual data challenges to discover lenses with both static and transient sources. For discovering lenses with static sources from large survey data, machine learning is currently the most popular method ([8], for a review). The prerequisite for this kind of data challenge is a realistic simulation pipeline. The SLSim pipeline[8] is currently being developed with that as one of its main goals [81]. An additional goal of this pipeline is to characterize the selection function of the discovered lenses, which will be essential to achieve most of the science goals described in §3. Therefore, the deflector and background source galaxy and transient populations are modelled in this pipeline with high realism based on empirical luminosity functions and scaling relations. This pipeline is also being developed with generalizability; thus, it will be easy to use it for similar purposes for *Euclid* or the *Roman* Space Telescope.

5. Summary

In this article, we provided an overview of the strong-lensing science cases enabled by the Rubin LSST. First, we briefly reviewed the forecasted number of different types of strong-lensing systems (§2). We then described some of the principal strong-lensing science cases to be achieved with the LSST-discovered strong-lensing samples, either utilizing the LSST data alone or with follow-up data obtained from other facilities (§3). We provided an updated forecast on constraining the dark energy equation-of-state parameters w_0 and w_a. In this forecast, we demonstrate that by combining the four strong-lens samples—lensed quasars with measured time delays, lensed

---

[4]https://sites.google.com/view/lsst-stronglensing.
[5]https://lsstdesc.org/
[6]SLTT is part of the Time-Domain Working Group in DESC.
[7]https://sitcomtn-050.lsst.io/
[8]https://github.com/LSST-strong-lensing/slsim

SNIae with measured time delays, single-plane lenses with kinematics and double-source-plane lenses—strong lensing will become the most constraining dark energy probe for the Rubin LSST. Finally, we described the current and near-future community efforts for timely preparation of the analysis pipelines in anticipation of the near-future arrival of the first real dataset from the Rubin LSST in 2026 (§4).

Appendix A. Settings for dark energy forecasts

Here, we describe the settings used in our forecast for Rubin LSST's strong-lensing constraints on the dark energy equation-of-state parameters. We use hierArc[9] to sample from the cosmological parameter posterior with emcee [83,94]. Below, we provide the specific sample and settings for each of the four strong-lensing probes of the dark energy. We assume space-based (from the HST, JWST, *Euclid* or *Roman*) or adaptive-optics-assisted ground-based imaging [95] to be used for lens modelling for the probes below. In addition to needing spectroscopic redshift measurements for all these probes, measured time delays will be necessary for the probes in (a) and (b), with velocity dispersion measurements being crucial for the probes in (b) and (c).

A.1. Time-delay cosmography with lensed SNIa

We adopt the mock sample of 144 lensed SNIa from [46]: 120 doubles and 24 quads with eight each in the cusp, cross and fold configurations. We only use the future *Roman* sample of unlensed SNIa from [46] to provide a prior constraint on the mean apparent magnitude $\overline{m}_{\rm p}$ at the pivot redshift $z_{\rm pivot} = 0.1$. In this forecast, we do not use the relative expansion history from this future *Roman* sample of unlensed SNIa so that the extracted cosmological constraints are only based on time-delay cosmography of the lensed SNIa sample.

---

[9]https://github.com/sibirrer/hierarc.

A.2. Time-delay cosmography with lensed quasars

We adopt a sample of 236 lensed quasars from the catalogue of [3] with variability amplitude more than three times the uncertainty achieved by LSST photometry, based on the estimation by [18]. This large threshold on the variability amplitude is conservative. Thus, this sample size can still be achieved with a lower threshold if the more conservative numbers based on the catalogue of [17] are considered. For example, 346 lenses from the [17] catalogue will have variability amplitude larger than the LSST photometric uncertainty (Y. C. Taak, private communication, 2024).

We assume 40 of these 236 systems to have JWST kinematics and the rest to have single-aperture kinematics measurements. The deflector and source redshifts of these lenses are obtained from the catalogue of [3]. We make the same assumptions as [47] for all the other settings in the forecast, including the resolution and uncertainty specifications of the kinematics. We add a population scatter with $\sigma = 0.025$ in the external convergence (κ_{ext}) for the lensed quasar systems on top of the settings of [47], to be self-consistent with the settings applied on the lensed SNIa sample from [46]. However, for both the lensed SNIa and quasar sample, the population mean and scatter of external convergence are fixed to their true values, since the magnification or the kinematics breaks the total (i.e. internal and external combined) mass-sheet degeneracy, thus leaving a perfect degeneracy between the mean internal mass-sheet-transform parameter $\overline{\lambda}_{int}$ and the mean external convergence $\overline{\kappa}_{ext}$ if both are freely varied. Following [47], we still assume a 2% uncertainty for each individual system's measurement of the external convergence that contributes toward the overall uncertainty on $\overline{\lambda}_{int}$.

A.3. Single-plane lenses with kinematics

We use the posterior for this sample of 10 000 lenses directly from [44]. When combining this probe with the other three, we use the kernel density estimate of this posterior as an additional prior term jointly applied on Ω_m, w_0 and w_a.

A.4. Double-source-plane lenses

We use the same sample of 87 double-source-plane lenses from [43,48] with the same redshift and β values. Although the full LSST dataset is forecasted to contain approximately 500 double-source-plane lenses, the number 87 corresponds to the ones identified from single-epoch images with the best seeing.

References

1. Allison J, Anderson SF, Andrew JR, Angel JRP, Armus L, LSST Science Collaborations. 2009 *LSST science book, Version 2.0. arXiv e-prints*. (doi:10.48550/arXiv.0912.0201)
2. Ivezić Ž, Kahn SM, Tyson JA, Abel B, Acosta E, Allsman R, Alonso D. 2019 LSST: from science drivers to reference design and anticipated data products. *Astrophys. J.* **873**, 111. (doi:10.3847/1538-4357/ab042c)
3. Oguri M, Marshall PJ. 2010 Gravitationally lensed quasars and supernovae in future wide-field optical imaging surveys. *Mon. Not. R. Astron. Soc.* **405**, 2579–2593. (doi:10.1111/j.1365-2966.2010.16639.x)
4. Collett TE. 2015 The population of galaxy-galaxy strong lenses in forthcoming optical imaging surveys. *Astrophys. J.* **811**, 20. (doi:10.1088/0004-637X/811/1/20)
5. Ferrami G, Wyithe JSB. 2024 A model for galaxy–galaxy strong lensing statistics in surveys. *Mon. Not. R. Astron. Soc.* **532**, 1832–1848. (doi:10.1093/mnras/stae1607)
6. Jacobs C *et al*. 2019 An extended catalog of galaxy–galaxy strong gravitational lenses discovered in DES using convolutional neural networks. *Astrophys. J. Suppl. Ser.* **243**, 17. (doi:10.3847/1538-4365/ab26b6)

7. Rojas K *et al*. 2023 The impact of human expert visual inspection on the discovery of strong gravitational lenses. *Mon. Not. R. Astron. Soc.* **523**, 4413–4430. (doi:10.1093/mnras/stad1680)

8. Lemon C *et al*. 2024 Searching for strong gravitational lenses. *Space Sci. Rev.* **220**, 23. (doi:10.1007/s11214-024-01042-9)

9. Marshall PJ *et al*. 2016 SPACE WARPS – I. Crowdsourcing the discovery of gravitational lenses. *Mon. Not. R. Astron. Soc.* **455**, 1171–1190. (doi:10.1093/mnras/stv2009)

10. Holloway P, Marshall PJ, Verma A, More A, Cañameras R, Jaelani AT, Ishida Y, Wong KC. 2024 A Bayesian approach to strong lens finding in the era of wide-area surveys. *Mon. Not. R. Astron. Soc.* **530**, 1297–1310. (doi:10.1093/mnras/stae875)

11. Goobar A *et al*. 2017 iPTF16geu: a multiply imaged, gravitationally lensed type Ia supernova. *Science* **356**, 291–295. (doi:10.1126/science.aal2729)

12. Goobar A *et al*. 2023 Uncovering a population of gravitational lens galaxies with magnified standard candle SN Zwicky. *Nat. Astron.* **7**, 1098–1107. (doi:10.1038/s41550-023-01981-3)

13. Goldstein DA, Nugent PE, Goobar A. 2019 Rates and properties of supernovae strongly gravitationally lensed by elliptical galaxies in time-domain imaging surveys. *Astrophys. J. Suppl. Ser.* **243**, 6. (doi:10.3847/1538-4365/ab1fe0)

14. Sainz de Murieta A, Collett TE, Magee MR, Weisenbach L, Krawczyk CM, Enzi W. 2023 Lensed type Ia supernovae in light of SN Zwicky and iPTF16geu. *Mon. Not. R. Astron. Soc.* **526**, 4296–4307. (doi:10.1093/mnras/stad3031)

15. Wojtak R, Hjorth J, Gall C. 2019 Magnified or multiply imaged? – Search strategies for gravitationally lensed supernovae in wide-field surveys. *Mon. Not. R. Astron. Soc.* **487**, 3342–3355. (doi:10.1093/mnras/stz1516)

16. Arendse N *et al*. 2024 Detecting strongly lensed type Ia supernovae with LSST. *Mon. Not. R. Astron. Soc.* **531**, 3509–3523. (doi:10.1093/mnras/stae1356)

17. Taak YC, Treu T. 2023 Strong lensed QSOs with variability detectable by LSST: how many are there? *Mon. Not. R. Astron. Soc.* **524**, 5446–5453. (doi:10.1093/mnras/stad2201)

18. Yue M, Fan X, Yang J, Wang F. 2022 A mock catalog of gravitationally-lensed quasars for the LSST survey. *Astron. J.* **163**, 139. (doi:10.3847/1538-3881/ac4cb0)

19. Abe KT, Oguri M, Birrer S, Khadka N, Marshall PJ, Lemon C, More A, LSST Dark Energy Science Collaboration. 2025. A halo model approach for mock catalogs of time-variable strong gravitational lenses. *Open J. Astrophys.* **8**. (doi:10.33232/001c.128482)

20. Refsdal S. 1964 On the possibility of determining Hubble's parameter and the masses of galaxies from the gravitational lens effect. *Mon. Not. R. Astron. Soc.* **128**, 307–310. (doi:10.1093/mnras/128.4.307)

21. Birrer S, Millon M, Sluse D, Shajib AJ, Courbin F, Erickson S, Koopmans LVE, Suyu SH, Treu T. 2024 Time-delay cosmography: measuring the Hubble constant and other cosmological parameters with strong gravitational lensing. *Space Sci. Rev.* **220**, 48. (doi:10.1007/s11214-024-01079-w)

22. Treu T, Shajib AJ. 2024 Strong lensing and H_0. In *The Hubble constant tension* (eds E Di Valentino, D Brout), pp. 251–276. Singapore: Springer Nature Singapore.

23. Millon M, Galan A, Courbin F, Treu T, Suyu SH, Ding X, Birrer S. 2020 TDCOSMO. I. An exploration of systematic uncertainties in the inference of H_0 from time-delay cosmography. *Astron. Astrophys.* **639**, A101. (doi:10.1051/0004-6361/201937351)

24. Birrer S, Shajib AJ, Galan A, Millon M, Treu T, Agnello A, Auger M. 2020 TDCOSMO - IV. Hierarchical time-delay cosmography – joint inference of the Hubble constant and galaxy density profiles. *Astron. Astrophys.* **643**, A165. (doi:10.1051/0004-6361/202038861)

25. Napier K, Sharon K, Dahle H, Bayliss M, Gladders MD, Mahler G, Rigby JR, Florian M. 2023 Hubble constant measurement from three large-separation quasars strongly lensed by galaxy clusters. *Astrophys. J.* **959**, 134. (doi:10.3847/1538-4357/ad045a)

26. Quimby RM *et al*. 2013 Extraordinary magnification of the ordinary type Ia supernova PS1-10afx. *Astrophys. J.* **768**, L20. (doi:10.1088/2041-8205/768/1/L20)

27. Kelly PL *et al*. 2015 Multiple images of a highly magnified supernova formed by an early-type cluster galaxy lens. *Science* **347**, 1123–1126. (doi:10.1126/science.aaa3350)

28. Kelly PL *et al*. 2023 Constraints on the Hubble constant from supernova Refsdal's reappearance. *Science* **380**, eabh1322. (doi:10.1126/science.abh1322)

29. Pascale M, L.Frye B, Pierel JDR, Chen W, L.Kelly P, H.Cohen S, A.Windhorst R. SN H0pe: the first measurement of H0 from a multiply-imaged type Ia supernova, discovered by JWST. *ApJ* **979**, 1–13. (doi:10.48550/arXiv.2403.18902)

30. Pierel JDR, Newman AB, Dhawan S, Gu M, Joshi BA, Li T, Schuldt S. 2024 Lensed type Ia supernova 'Encore' at z = 2: the first instance of two multiply imaged supernovae in the same host galaxy. *Astrophys. J. Lett*. **967**, L37. (doi:10.3847/2041-8213/ad4648)

31. Shajib AJ, Treu T, Agnello A. 2018 Improving time-delay cosmography with spatially resolved kinematics. *Mon. Not. R. Astron. Soc*. **473**, 210–226. (doi:10.1093/mnras/stx2302)

32. Shajib AJ, Mozumdar P, Chen GCF, Treu T, Cappellari M, Knabel S, Suyu SH. 2023 TD-COSMO. XII. Improved Hubble constant measurement from lensing time delays using spatially resolved stellar kinematics of the lens galaxy. *Astron. Astrophys*. **673**, A9. (doi:10.1051/0004-6361/202345878)

33. Huber S, Suyu SH, Noebauer UM, Bonvin V, Rothchild D, Chan JHH, Awan H. 2019 Strongly lensed SNe Ia in the era of LSST: observing cadence for lens discoveries and time-delay measurements. *Astron. Astrophys*. **631**, A161. (doi:10.1051/0004-6361/201935370)

34. Ding X, Liao K, Birrer S, Shajib AJ, Treu T, Yang L. 2021 Improved time-delay lens modelling and H_0 inference with transient sources. *Mon. Not. R. Astron. Soc*. **504**, 5621–5628. (doi:10.1093/mnras/stab1240)

35. Schneider P, Ehlers J, Falco EE. 1992 *Gravitational lenses*. Berlin, Heidelberg: Springer. (doi:10.1007/978-3-662-03758-4)

36. Golse G, Kneib JP. 2002 Pseudo elliptical lensing mass model: application to the NFW mass distribution. *Astron. Astrophys*. **390**, 821–827. (doi:10.1051/0004-6361:20020639)

37. Jullo E, Natarajan P, Kneib JP, D'Aloisio A, Limousin M, Richard J, Schimd C. 2010 Cosmological constraints from strong gravitational lensing in clusters of galaxies. *Science* **329**, 924–927. (doi:10.1126/science.1185759)

38. Collett TE, Auger MW, Belokurov V, Marshall PJ, Hall AC. 2012 Constraining the dark energy equation of state with double-source plane strong lenses. *Mon. Not. R. Astron. Soc*. **424**, 2864–2875. (doi:10.1111/j.1365-2966.2012.21424.x)

39. Kneib JP, Natarajan P. 2011 Cluster lenses. *Astron. Astrophys. Rev*. **19**, 47. (doi:10.1007/s00159-011-0047-3)

40. Gavazzi R, Treu T, Koopmans LVE, Bolton AS, Moustakas LA, Burles S, Marshall PJ. 2008 The Sloan Lens ACS survey. VI. Discovery and analysis of a double Einstein ring. *Astrophys. J*. **677**, 1046–1059. (doi:10.1086/529541)

41. Tanaka M, Wong KC, More A, Dezuka A, Egami E, Oguri M, Suyu SH. 2016 A spectroscopically confirmed double source plane lens system in the hyper suprime-cam subaru strategic program. *Astrophys. J. Lett*. **826**, L19. (doi:10.3847/2041-8205/826/2/L19)

42. Shajib AJ, Birrer S, Treu T, Agnello A, Buckley-Geer EJ, Chan JHH, Christensen L. 2020 STRIDES: a 3.9 per cent measurement of the Hubble constant from the strong lens system DES J0408-5354. *Mon. Not. R. Astron. Soc*. **494**, 6072–6102. (doi:10.1093/mnras/staa828)

43. DESC, Mandelbaum R, Eifler T, Hložek R, Collett T, Gawiser E, Scolnic D. The LSST Dark Energy Science Collaboration (DESC) science requirements document. *arXiv e-print*. (doi:10.48550/arXiv.1809.01669)

44. Li T, Collett TE, Krawczyk CM, Enzi W. 2024 Cosmology from large populations of galaxy-galaxy strong gravitational lenses. *Mon. Not. R. Astron. Soc*. **527**, 5311–5323. (doi:10.1093/mnras/stad3514)

45. Collett TE, Sonnenfeld A, Frohmaier C, Glazebrook K, Sluse D, Motta V, Verma A. 2023 The 4MOST Strong Lensing Spectroscopic Legacy Survey (4SLSLS). *Messenger* **190**, 49–52. (doi:10.18727/0722-6691/5313)

46. Birrer S, Dhawan S, Shajib AJ. 2022 The Hubble constant from strongly lensed supernovae with standardizable magnifications. *Astrophys. J*. **924**, 2. (doi:10.3847/1538-4357/ac323a)

47. Birrer S, Treu T. 2021 TDCOSMO. V. Strategies for precise and accurate measurements of the Hubble constant with strong lensing. *Astron. Astrophys*. **649**, A61. (doi:10.1051/0004-6361/202039179)

48. Sharma D, Collett TE, Linder EV. 2023 Testing cosmology with double source lensing. *J. Cosmol. Astropart. Phys*. **2023**, 001. (doi:10.1088/1475-7516/2023/04/001)

49. Albrecht A, Bernstein G, Cahn R, Freedman W, Hewitt J, Hu W, Huth J. 2006 Report of the dark energy task force. *arXiv e-print*. (doi:10.48550/arXiv.astro-ph/0609591)

50. Khadka N, Birrer S, Leauthaud A, Nix H. 2024 Breaking the mass-sheet degeneracy in strong lensing mass modelling with weak lensing observations. *Mon. Not. R. Astron. Soc*. **533**, 795–806. (doi:10.1093/mnras/stae1832)

51. Vegetti S *et al*. 2024 Strong gravitational lensing as a probe of dark matter. *Space Sci. Rev.* **220**, 58. (doi:10.1007/s11214-024-01087-w)

52. Mao S, Schneider P. 1998 Evidence for substructure in lens galaxies? *Mon. Not. R. Astron. Soc.* **295**, 587–594. (doi:10.1046/j.1365-8711.1998.01319.x)

53. Koopmans LVE. 2005 Gravitational imaging of cold dark matter substructures. *Mon. Not. R. Astron. Soc.* **363**, 1136–1144. (doi:10.1111/j.1365-2966.2005.09523.x)

54. Vegetti S, Koopmans LVE. 2009 Bayesian strong gravitational-lens modelling on adaptive grids: objective detection of mass substructure in Galaxies. *Mon. Not. R. Astron. Soc.* **392**, 945–963. (doi:10.1111/j.1365-2966.2008.14005.x)

55. Daylan T, Cyr-Racine FY, Rivero AD, Dvorkin C, Finkbeiner DP. 2018 Probing the small-scale structure in strongly lensed systems via transdimensional inference. *Astrophys. J.* **854**, 141. (doi:10.3847/1538-4357/aaaa1e)

56. Despali G, Vegetti S, White SDM, Powell DM, Stacey HR, Fassnacht CD, Rizzo F, Enzi W. 2022 Detecting low-mass haloes with strong gravitational lensing I: the effect of data quality and lensing configuration. *Mon. Not. R. Astron. Soc.* **510**, 2480–2494. (doi:10.1093/mnras/stab3537)

57. Dvorkin C, Ostdiek B, Tsang A. 2022 Substructure detection reanalysed: dark perturber shown to be a line-of-sight halo. Mon. Not. R. Astron. Soc. **515**, 4391–4401. (doi:10.1093/mnras/stac1967)

58. Gilman D, Birrer S, Treu T, Nierenberg A, Benson A. 2019 Probing dark matter structure down to 107 solar masses: flux ratio statistics in gravitational lenses with line-of-sight haloes. *Mon. Not. R. Astron. Soc.* **487**, 5721–5738. (doi:10.1093/mnras/stz1593)

59. Hezaveh Y, Dalal N, Holder G, Kisner T, Kuhlen M, Levasseur LP. Measuring the power spectrum of dark matter substructure using strong gravitational lensing. *J. Cosmol. Astropart. Phys.* **2016**, 048–048. (doi:10.1088/1475-7516/2016/11/048)

60. Bolton AS, Burles S, Koopmans LVE, Treu T, Gavazzi R, Moustakas LA, Wayth R, Schlegel DJ. 2008 The Sloan Lens ACS survey. V. The full ACS strong-lens sample. *Astrophys. J.* **682**, 964–984. (doi:10.1086/589327)

61. Daylan T, Birrer S. 2023 Searching for dark matter substructure: a deeper wide-area community survey for roman. *arXiv*. (doi:10.48550/arXiv.2306.12864). See https://arxiv.org/abs/2306.12864.

62. Keeley RE, Nierenberg AM, Gilman D, Birrer S, Benson AJ, 2024 JWST lensed quasar dark matter survey - II. Strongest gravitational lensing limit on the dark matter free streaming length to date. *Mon. Not. R. Astron. Soc* **535**, 1652–1671. (doi:10.1093/mnras/stae2458)

63. Natarajan P, Williams LLR, Bradač M, Grillo C, Ghosh A, Sharon K, Wagner J. 2024 Strong lensing by galaxy clusters. *Space Sci. Rev.* **220**, 19. (doi:10.1007/s11214-024-01051-8)

64. Elbert OD, Bullock JS, Kaplinghat M, Garrison-Kimmel S, Graus AS, Rocha M. 2018 A testable conspiracy: simulating baryonic effects on self-interacting dark matter halos. *Astrophys. J.* **853**, 109. (doi:10.3847/1538-4357/aa9710)

65. Kong D, Yang D, Yu HB. 2024 Cold dark matter and self-interacting dark matter interpretations of the strong gravitational lensing object JWST-ER1. *Astrophys. J. Lett.* **965**, L19. (doi:10.3847/2041-8213/ad394b)

66. de Blok WJG. 2010 The core-cusp problem. *Adv. Astron.* **2010**, 1–14. (doi:10.1155/2010/789293)

67. Bullock JS, Boylan-Kolchin M. 2017 Small-scale challenges to the ΛCDM paradigm. *Annu. Rev. Astron. Astrophys.* **55**, 343–387. (doi:10.1146/annurev-astro-091916-055313)

68. Drlica-Wagner A, Mao YY, Adhikari S, Armstrong R, Banerjee A, Banik N, Bechtol K. 2019 Probing the fundamental nature of dark matter with the Large Synoptic Survey Telescope. *arXiv e-print*. (doi:10.48550/arXiv.1902.01055)

69. Diego JM, Bernstein G, Chen W, Goobar A, Johansson JP, Kelly PL, Mörtsell E, Nightingale JW. 2022 Microlensing and the type Ia supernova iPTF16geu. *Astron. Astrophys.* **662**, A34. (doi:10.1051/0004-6361/202143009)

70. Arendse N *et al*. In preparation

71. Shajib AJ *et al*. 2024 Strong lensing by galaxies. *Space Sci. Rev.* **220**, 87. (doi:10.1007/s11214-024-01105-x)

72. Treu T, Suyu SH, Marshall PJ. 2022 Strong lensing time-delay cosmography in the 2020s. *Astron. Astrophys. Rev.* **30**. (doi:10.1007/s00159-022-00145-y)

73. Vernardos G *et al*. 2024 Microlensing of Strongly Lensed Quasars. *Space Sci. Rev.* **220**, 14. (doi:10.1007/s11214-024-01043-8)

13

royalsocietypublishing.org/journal/rsta   *Phil. Trans. R. Soc. A* **383:** 20240117

74. Suyu SH, Goobar A, Collett T, More A, Vernardos G. 2024 Strong Gravitational Lensing and Microlensing of Supernovae. *Space Sci. Rev.* **220**, 13. (doi:10.1007/s11214-024-01044-7)

75. Schechter PL, Pooley D, Blackburne JA, Wambsganss J. 2014 A calibration of the stellar mass fundamental plane at z ∼ 0.5 using the micro-lensing-induced flux ratio anomalies of macro-lensed quasars. *ApJ* **2**, 96. (doi:10.1088/0004-637X/793/2/96)

76. Neira F, Anguita T, Vernardos G. 2020 A quasar microlensing light-curve generator for LSST. *Mon. Not. R. Astron. Soc.* **495**, 544–553. (doi:10.1093/mnras/staa1208)

77. Oguri M. 2019 Strong gravitational lensing of explosive transients. *Rep. Prog. Phys.* **82**, 126901. (doi:10.1088/1361-6633/ab4fc5)

78. Ryczanowski D, Smith GP, Bianconi M, Massey R, Robertson A, Jauzac M. 2020 On building a cluster watchlist for identifying strongly lensed supernovae, gravitational waves and kilonovae. *Mon. Not. R. Astron. Soc.* **495**, 1666–1671. (doi:10.1093/mnras/staa1274)

79. Ryczanowski D, Smith GP, Bianconi M, McGee S, Robertson A, Massey R, Jauzac M. 2023 Enabling discovery of gravitationally lensed explosive transients: a new method to build an all-sky watch list of groups and clusters of galaxies. *Mon. Not. R. Astron. Soc.* **520**, 2547–2557. (doi:10.1093/mnras/stad231)

80. Smith GP, Anguita T, Birrer S, L.Schechter P, Verma A, Collett T, Courbin F. 2021 Strong Lensing Science Collaboration input to the on-sky commissioning of the Vera Rubin Observatory. *arXiv e-print*. (doi:10.48550/arXiv.2111.09216)

81. Khadka N *et al.* In preparation.

82. ajshajib. 2024 dark_energy_forecast_rubin_strong_lensing. GitHub https://github.com/ajshajib/dark_energy_forecast_rubin_strong_lensing

83. Foreman-Mackey D, Hogg DW, Lang D, Goodman J. 2013 Emcee: the MCMC hammer. *Publ. Astron. Soc. Pac.* **125**, 306–312. (doi:10.1086/670067)

84. Birrer S, Amara A. 2018 *lenstronomy*: multi-purpose gravitational lens modelling software package. *Phys. Dark Universe* **22**, 189–201. (doi:10.1016/j.dark.2018.11.002)

85. Birrer S, Shajib AJ, Gilman D, Galan A, Aalbers J, Millon M, Morgan R. 2021 Lenstronomy II: a gravitational lensing software ecosystem. *J. Open Source Softw*. **6**, 3283. (doi:10.21105/joss.03283)

86. Oliphant TE. 2015 *Guide to numpy*, 2nd edition. North Charleston, SC: CreateSpace Independent Publishing Platform.

87. Robitaille TP *et al*. 2013 Astropy: a community python package for astronomy. *A&A* **558**, A33. (doi:10.1051/0004-6361/201322068)

88. Astropy Collaboration. 2018 The astropy project: building an open-science project and status of the v2.0 core package. *Astron. J*. **156**, 123. (doi:10.3847/1538-3881/aabc4f)

89. Astropy Collaboration. 2022 The astropy project: sustaining and growing a community-oriented open-source project and the latest major release (v5.0) of the core package. *Astrophys. J*. **935**, 167. (doi:10.3847/1538-4357/ac7c74)

90. Pedregosa F, Varoquaux G, Gramfort A, Michel V, Thirion B, Grisel O, Blondel M. 2011 Scikit-learn: machine learning in Python. *J. Mach. Learn. Res*. **12**, 2825–2830. http://jmlr.org/papers/v12/pedregosa11a.html

91. Hunter JD. 2007 Matplotlib: a 2D graphics environment. *Comput. Sci. Eng*. **9**, 90–95. (doi:10.1109/MCSE.2007.55)

92. Hinton SR. 2016 ChainConsumer. *JOSS* **1**, 45. (doi:10.21105/joss.00045)

93. Waskom M, Botvinnik O, Hobson P, B.Cole J, Halchenko Y, Hoyer S, Miles A. 2014 Seaborn:v0.5.0. Zenodo. (doi:10.5281/zenodo.12710)

94. Goodman J, Weare J. 2010 Ensemble samplers with affine invariance. *Commun. Appl. Math. Comput. Sci*. **5**, 65–80. (doi:10.2140/camcos.2010.5.65)

95. Chen GCF *et al*. 2019 A SHARP view of H0LiCOW: H_0 from three time-delay gravitational lens systems with adaptive optics imaging. *Mon. Not. R. Astron. Soc*. **490**, 1743–1773. (doi:10.1093/mnras/stz2547)